HHS Public Access

Author manuscript

Exp Eye Res. Author manuscript; available in PMC 2017 September 01.

Published in final edited form as:

Exp Eye Res. 2016 September ; 150: 81–89. doi:10.1016/j.exer.2015.05.013.

Aberrant activity in retinal degeneration impairs central visual processing and relies on Cx36-containing gap junctions

Elena Ivanova, **Christopher W Yee**, **Robert Baldoni Jr.**, and **Botir T Sagdullaev**

Departments of Ophthalmology and Neurology, Weill Medical College of Cornell University, Burke Medical Research Institute, White Plains, NY 10605

Abstract

In retinal degenerative disease (RD), the diminished light signal from dying photoreceptors has been considered the sole cause of visual impairment. Recent studies show a 10-fold increase in spontaneous activity in the RD network, challenging this paradigm. This aberrant activity forms a new barrier for the light signal, and not only exacerbates the loss of vision, but also may stand in the way of visual restoration. This activity originates in AII amacrine cells and relies on excessive activation of gap junctions. However, it remains unclear whether aberrant activity affects central visual processing and what mechanisms lead to this excessive activation of gap junctions. By combining genetic manipulation with electrophysiological recordings of light-induced activity in both living mice and isolated wholemount retina, we demonstrate that aberrant activity extends along retinotectal projections to alter activity in higher brain centers. Next, to selectively eliminate Cx36-containing gap junctions, which are the primary type expressed by AII amacrine cells, we crossed *rd10* mice, a slow-degenerating model of RD, with Cx36 knockout mice. We found that retinal aberrant activity was reduced in the *rd10*/*Cx36*KO mice compared to *rd10* controls, a direct evidence for involvement of Cx36-containing gap junctions in generating aberrant activity in RD. These data provide an essential support for future experiments to determine if selectively targeting these gap junctions could be a valid strategy for reducing aberrant activity and restoring light responses in RD.

Keywords

retinal degeneration; retinal remodeling; superior colliculus; connexin36; rd10

Introduction

The fundamental task of any sensory system is to extract a meaningful signal from surrounding noise. In the retina, this is accomplished at multiple levels: individual cells amplify their signal, while network interactions reduce noise. Preserving this balance is imperative for retinal function (Dunn et al., 2006).

Corresponding Author: Botir T. Sagdullaev, 785 Mamaroneck Ave., White Plains, NY 10605, bos2005@med.cornell.edu.

During retinal degenerative disease (RD), such as retinitis pigmentosa, diminished visual signal from dying photoreceptor cells has been considered the sole cause of impairment. Recent studies, however, cast new light to our understanding by revealing that functional changes within surviving retina lead to the emergence of aberrant neuronal activity. In particular, we found that this aberrant activity lowers signal fidelity in RD, exacerbating the visual deficit (Yee et al., 2014). Selectively reducing this activity by blocking gap junctions increases sensitivity to signals from surviving photoreceptors, and enhances the responses to electrical stimulation of the surviving retina (Toychiev et al., 2013a). These findings establish the aberrant network as a novel target for treating RD, advancing therapeutic strategies beyond the paradigm of replacing the function of lost photoreceptors. Aberrant activity disrupts visual signaling in the retina; however, whether this activity affects responses in higher visual centers is unclear. This is important since, if this activity goes beyond the retina, it would have major impact on visual perception in patients with RD. Such a deficit has been previously observed in higher visual centers (Drager and Hubel, 1978), suggesting that the degradation of signal fidelity that occurs in the retina may translate to visual impairment, though this observation has not been explored beyond this single study, to our knowledge.

Here, we provide further support for this possibility by recording the activity in retinotectal projections in living mice. This approach has several major advantages. Around 70% of retinal ganglion cells (RGCs) in mouse retina project their axons directly to cells in the superficial layer of the SC (Hofbauer and Drager, 1985) and do so in a retinotopic manner: each area of the SC has a corresponding region in the retina (O'Leary and McLaughlin, 2005). Therefore, the same area of the visual field may be tested across experimental animals by targeting the same SC coordinates. This is particularly important for RD, as degeneration is typically more advanced in central versus peripheral areas. On a technical note, the SC is a distinct structure that can be targeted following a brief surgery without an overreliance on stereotaxic coordinates. In recordings from cells in superficial layers of superior colliculus of *rd10* mice, a well-established slow-degenerating model of retinitis pigmentosa, we found the presence of aberrant activity that strongly resembles the aberrant activity in RGCs.

In the retina, aberrant activity originates in AII amacrine cells and relies on excessive activation of gap junctions (Trenholm et al., 2012; Choi et al., 2014). Since AII amacrine cell gap junctions are comprised of Cx36 (Deans et al., 2002), we next hypothesized that genetic deletion of Cx36 would reduce aberrant hyperactivity in RD RGCs. This has not been tested directly, since there is no specific blocker of Cx36. Here, to selectively eliminate Cx36-containing gap junctions, we crossed *rd10* mice with Cx36 knockout mice. We found that aberrant hyperactivity was reduced in the *rd10*/Cx36 mice compared to *rd10* controls. These data provides direct evidence for involvement of Cx36-containing gap junctions in generating aberrant activity in RD.

Methods

Animals

In all experimental procedures, animals were treated according to regulations in the ARVO Statement for the Use of Animals in Ophthalmic and Vision Research, in accordance with protocols approved by the Institutional Animal Care and Use Committee of Weill Cornell Medical College, and the NIH Guide for the Care and Use of Laboratory Animals. Wildtype (RRID:IMSR_JAX:000664) and *rd10* (RRID:MGI_3581193) mice of either sex between 45-140 days old were obtained from the Jackson Laboratory (Bar Harbor, ME). *Cx36*$^{-/-}$ mice (Gjd2tm1Paul RRID:MGI_3810172) were kindly provided by David Paul (Harvard Medical School, Boston, MA).

Genotyping

Genotyping was performed by PCR on tail-extracted DNA. *rd10* PCR was conducted as previously described (Chang et al., 2007; Mazzoni et al., 2008). The primers to detect mutated Pde6b (*Pde6b*^{rd10}) were as follows: *RD10* F (CTTTCTATTCTCTGTCAGCAAAGC) and *RD10* R (CATGAGTAGGGTAAACATGGTCTG). The corresponding PCR amplification was performed by denaturation at 94°C for 3 min; annealing at 94, 60, and 72°C, respectively, for 1 min, 30 s, and 1 min for 30 cycles, and elongation at 72°C for 7 min. The product obtained was purified and digested with the NarI or Hhal enzymes (New England Biolabs), whose restriction site is not included in the *rd10* mutant DNA. The digested DNA was run on a 4.5% agarose gel (Bio-Rad) for separation of short DNA fragments. The homozygous *rd10* mutation is revealed by the presence of a single band having a size of 97 bp. *Cx36*$^{-/-}$ mice were identified based on PCR analysis (Deans et al., 2001). Primers for *wt* (fwd AGCGGAGGGAGCAAACGAGAAG, rev CTGCCGAAATTGGGAACACTGAC) and knockout (fwd TCCGGCCGCTTGGGTGGAG, rev CAGGTAGCCGGATCAAGCGTATGC) alleles generated products of 533 bp and 360 bp, respectively. The corresponding PCR amplification was performed by denaturation at 94°C for 4 min; annealing at 94, 61, and 72°C, respectively, for 15 s, 20 s, and 45 s for 31 cycles, and elongation at 72°C for 8 min. A new line of *Cx36*$^{-/-}$/*Pde6bβ*^{rd10} mice, from here on named *rd10/Cx36*$^{-/-}$, was obtained by crossing homozygous *rd10* with homozygous *Cx36*$^{-/-}$ mice. The *rd10/Cx36*$^{-/-}$ mice deficient for both *Cx36*$^{-/-}$and *Pde6b*^{rd10} genes were identified after two consequent PCR rounds for *Cx36*$^{-/-}$and *Pde6b*^{rd10}, respectively.

Preparation of retinal wholemounts

Methods for wholemount tissue preparation have been described in detail previously (Toychiev et al., 2013b). After the animal was euthanized, its eyes were enucleated and placed in bicarbonate-buffered Ames solution, constantly equilibrated with 95% O_2 and 5% CO_2. The cornea, iris and lens were removed. The retina was dissected into four equal quadrants. Quadrants were attached photoreceptor surface down to a modified Millicell filter (Millipore, Bedford, MA). This preparation was transferred to a recording chamber on the stage of an upright Nikon FN1 microscope equipped with Hoffman modulation contrast optics (Modulation Optics, Inc.; Greenvale, NY). The recording chamber was constantly bathed (1 ml/min) with bicarbonate-buffered Ames solution, constantly equilibrated with

95% O_2 and 5% CO_2. Pharmacological agents were applied using an eight-channel superfusion system (Warner Instruments, Hamden, CT). All experiments were performed at a temperature of 32°C. All reagents were obtained from Sigma (St. Louis, MO) or Tocris (Minneapolis, MN).

In vitro recordings

To compare RGCs of similar classes, alpha-like RGCs were targeted based on large soma size and number of primary dendritic processes. In some instances, to increase the number of matched RGC classes across control and *rd10* groups, mice homozygous for the Thy1-YFP allele (B6.Cg-Tg(thy1-YFP)/J with genetically prelabeled RGCs were used as control. Extracellular spiking activity was obtained from RGCs in a loose-patch mode using the electrode filled with HEPES-buffered extracellular Ringer's solution, containing the following (in mM): 137 NaCl, 2.5 KCl, 2.5 CaCl2, 1.0 MgCl2, 10 Na-HEPES, 28 glucose, pH 7.4. Electrodes were pulled from borosilicate glass (1B150F-4; WPI, Sarasota, FL) with a P-97 Flaming/Brown puller (Sutter Instruments, Novato, CA) and had a measured resistance of ~4-7 MΩ. All recordings were made with a MultiClamp 700B patch-clamp amplifier (Molecular Devices, Sunnyvale, CA) using Signal (CED, UK). Data were filtered at 5 kHz with a four-pole Bessel filter and were sampled at 15 kHz. After recordings, the cellular membrane under the pipette was ruptured to allow dye filling of the cell for morphological phenotyping.

Cell identification

The pipette solution was supplemented with 0.05% sulforhodamine B or Alexa Fluor 568 hydrazide to visualize non-prelabeled cells. Contrast and fluorescent images of the cell were documented with a modified Nikon D5000 DSLR attached to the microscope. The preparation was immediately placed into a glass bottom culture dish (MatTek, Ashland, MA) and transferred to the stage of a Nikon C-1 confocal microscope. A *z*-stack of 160 images was acquired at 0.5 um steps at a resolution of 1024x1024 pixels. Dendritic stratification was measured relative to the proximal (0%) to the distal margins (100%) of the IPL. In general, ON cells were defined as stratifying at <60%, with OFF cells stratifying at >60% of IPL depth. The precise depth of RGC dendritic stratification was confirmed by immunostaining against choline acetyl transferase (goat anti-ChAT, 1:2000; Chemicon).

Retinal stimulation and analysis

Light and electrical stimulation were both performed in wholemount retina. The microscope's illuminator was used to deliver a 200 μm spot of light centered on the RGC. An aperture, a series of neutral density (ND) filters, the FN-C LWD condenser (Nikon), and a Uniblitz shutter (Vincent Associates) were respectively used to control the size, intensity, focal plane, and duration of the stimulus. Stimulation routines were controlled by Signal 2 software (CED). The tissue was light adapted at 30 cd/m^2. For electrical stimulation, a positive current pulse (2 ms, 0.003-1.0 mA; Grass Technologies, Warwick, RI) was applied to the BCs in outer plexiform layer (OPL) using a patch pipette filled with extracellular solution. The stimulating electrode was first inserted into the BC layer. Once the stimulating electrode was stable, and the retinal tissue had settled (2–3 minutes), the RGC above was targeted for recordings.

In vivo recordings

To determine how retinal aberrant activity affects activity in higher visual centers, we recorded extracellular single unit responses from cells in superficial layer of SC (~ 300 μm deep) of *rd10*, and *wt* mice, using established procedures (Sagdullaev et al., 2006). An anesthetized mouse (1.5%–2.5% isoflurane) was placed in a stereotaxic frame. Eyes were dilated and protected with a zero power contact lens (Sagdullaev et al., 2003). A craniotomy was performed to expose the SC. Activity of individual cells was recorded with a tungsten electrode (WPI, Sarasota, FL). Using spots of light, responses were mapped to retinal locations.

Immunohistochemistry

The presence of Cx36 was analyzed in retinal wholemounts prepared as previously described (Ivanova et al., 2013). Briefly, living retinas were isolated from the eye cups and mounted onto modified Biopore filter as described for patch-clamp recordings. The retinas attached to the filter were submersion-fixed in freshly prepared 4% carbodiimide in 0.1 M phosphate saline (PBS, pH = 7.3) for 15 minutes. Retinal wholemounts were blocked for 1 h in a PBS solution containing 5% Chemiblocker (membrane-blocking agent, Chemicon), 0.5% Triton X-100, and 0.05% sodium azide (Sigma). Primary antibodies were diluted in the same solution and applied for 72 h, followed by incubation for 48 h in the appropriate secondary antibody, conjugated to Alexa 488 (1:1000; green fluorescence, Molecular Probes), Alexa 568 (1:1000; red fluorescence, Molecular Probes). In multi-labeling experiments, sections were incubated in a mixture of primary antibodies, followed by a mixture of secondary antibodies. All steps were carried out at room temperature. After staining, the retina was flat mounted on a slide, ganglion cell layer up, and coverslipped using Vectashield mounting medium (H-1000, Vector Laboratories). The coverslip was sealed in place with nail polish. To avoid extensive squeezing and damage to the retina, small pieces of a broken glass cover slip (Number 1 size) were placed in space between the slide and the coverslip. The Alexa 568 fluorescence was sufficient to visualize the Alexa 568-filled neurons, without antibody enhancement. The primary antibodies used in this study were the following: goat anti-ChAT (1:2000, Millipore Cat# AB144P RRID:AB_2079751), mouse anti-Cx36 (1:1000, Millipore Cat# MAB3045 RRID:AB_94632), and anti-GlyT1 (1:10000, Millipore Cat# AB1770 RRID:AB_90893).

Neurobiotin loading

For cut-loading, the retinas were dissected in oxygenated HEPES-buffered extracellular solution and cut into four quarters. Each quarter was attached to a nitrocellulose membrane. The radial cuts were made by a razor blade dipped into Neurobiotin powder (Vector Laboratories). The cuts were rinsed and incubated in HEPES-buffered extracellular solution for 50 min. To block gap junctions, the retinal tissue was pre-incubated for 10 min in meclofenamic acid (MFA, 100 μM). The tissue was kept in MFA solution until it was fixed. After fixation in 4% paraformaldehyde 0.1 M PBS, retinal quarters with cuts were removed from the nitrocellulose filter. Neurobiotin was visualized with Streptavidin-Cy3 (1:600) applied in a similar way as the primary antibody. All images were captured using a Nikon

C1 confocal microscope. The images were semi-automatically analyzed using ImageJ software.

Data analysis

Statistical analyses were performed using SigmaPlot (RRID:SciRes_000184, Systat Software Inc.) and SPSS (RRID:rid_000042, IBM). Student's or paired t-tests were used for group comparisons, and one-way analysis of variance (ANOVA) with Bonferroni post hoc tests for multiple comparisons, unless otherwise specified. Data are presented as mean ± standard error (SEM).

Results

Aberrant activity precludes transmission of evoked responses in RD

Structural changes to the surviving retina postsynaptic to photoreceptors have been well known for several decades, but the details of functional changes have only emerged relatively recently. The hallmark of these changes is the emergence of aberrant activity in numerous neurons within the inner retina (Marc et al., 2007; Stasheff, 2008). In the *rd10* mouse model of retinitis pigmentosa, RGCs spontaneously fire groups of action potentials, or "bursts" (Fig. 1A), in contrast to *wt* RGCs, which exhibit far less spontaneous spiking. There is a strong inverse correlation between basal spiking activity and the fidelity of the evoked responses in RD retina (Toychiev et al., 2013a); however, its impact on the processing of light-induced activity is unclear. In particular, given the ability of the retina to extract a useful signal from noise, this activity may not have a strong disruptive effect on the transmission of the visual signal. Alternatively, if the temporal structure of aberrant retinal activity is similar to the evoked response, it will impede the signal from surviving photoreceptors as it travels through the inner retina. To test this, we recorded spiking activity in loose-patch mode from identified RGCs in *wt* and age-matched *rd10* retinal wholemounts. In early RD (~P40), when a significant number of photoreceptor cells are still alive and functional, a brief light stimulus produced a noticeable increase in RGC firing rate (Fig. 1B, top). In late stages of RD, when photoreceptors are mostly absent, we applied focal electrical stimuli delivered to presynaptic bipolar cells, as illustrated for *wt* and *rd10* RGC in P140 mice (Fig. 1B, bottom). The majority of RGCs responded to stimuli by briefly increasing their firing rate, or during so-called transient response component. To account for this, we have measured the instantaneous frequency of firing (*F*i), defined here as the inverse time interval between an event and the previous one. To determine how aberrant activity during RD may affect stimulus-driven signal, instantaneous frequency firing rates were plotted for both evoked and spontaneous time epochs (Fig. 1C). In *wt* control RGCs, light stimuli produced a >30-fold change in *F*i (5.25 ± 0.7 to 154.43 7.36 Hz, n = 27 RGCs from 3 animals; $p < 0.001$). This is in contrast to *rd10* RGCs, in which stimuli produced no significant change in *F*i (102.66 ± 4.78 to 107.22 ± 14.61 Hz, n = 25 RGCs from 3 animals; $p = 0.74$). Thus, in *rd10* RGCs, the *F*i of spontaneous bursts is not significantly different from the *F*i of light-evoked responses. This suggests that *rd10* RGCs cannot reliably differentiate spontaneous activity from evoked responses, and that reducing spontaneous bursting will restore this distinction. To test for this, we selectively blocked aberrant bursting activity in *rd10* RGCs by including meclofenamic acid (MFA, 50 μM) into the bathing

solution. This treatment has been shown to target gap junctions in AII amacrine cells, a pacemaker of the aberrant activity (Trenholm et al., 2012; Choi et al., 2014). Indeed, MFA had an effect of reducing the *F*i of spontaneous bursts in *rd10* RGCs and significantly improved the discrimination of light-evoked activity (17.52 ± 4.36 to 93.93 ± 9.78 Hz, n = 15; $p < 0.0001$). This data provide strong evidence that the resting activity in RD retina is conflated with light responses.

Aberrant activity is present in retinal targets in the brain

While aberrant activity impairs retinal function, it remains unclear whether this activity is an impediment to light sensitivity in higher visual centers. This is important since, if this activity goes beyond the retina, it would have major impact on visual perception in patients with RD. To address this, we targeted the superior colliculus (SC) in living mice to determine whether retinal aberrant activity impacts higher visual centers. This approach has several major advantages. Around 70% of RGCs in mouse retina project their axons directly to cells in the superficial layer of the SC (Hofbauer and Drager, 1985) and do so in a retinotopic manner: each area of the SC has a corresponding region in the retina (O'Leary and McLaughlin, 2005). The rate of RD and corresponding changes to retinal function vary across different retinal regions; more advanced in central versus peripheral retina. Therefore, when comparing the properties of retinal signaling to brain targets across different animals it is important to consider the inputs arriving for similar retinal regions. The presence of a precise retinotopic map enables this comparison. To determine how retinal aberrant activity affects light-evoked responses in higher visual centers, we recorded extracellular single unit responses *in vivo* from cells in the superficial layer of the SC (~300 μm deep) in *rd10* and *wt* mice using previously established procedures (Sagdullaev et al., 2003; 2006; see Methods). Spontaneous activity in *rd10* SC cells was compared to identical locations in age-matched *wt* controls. Wildtype SC cells exhibited a low rate of spontaneous activity, similar to what was observed in *wt* RGCs (Fig. 2A, top). In contrast, *rd10* SC cells had prominent aberrant hyperactivity, exhibiting 4–10 Hz bursting, similar to the rate of bursting observed in *rd10* RGCs. Furthermore, this aberrant activity also interfered with responses driven by retinal light stimulation (Fig. 2A, bottom). Overall, spontaneous activity in rd10 SC cells (20.48 ± 1.94, n = 29, 3 animals) was significantly greater than in wt SC cells (6.10 ± 0.99, n = 29, 3 animals; $p < 0.0001$, Fig. 2B). This data reveal aberrant activity in the SC neurons of *rd10* mice, providing evidence that RD dysfunction is not limited to retina and may impair visual activity in higher brain centers.

Cx36-containing gap junctions are essential for aberrant activity in RD

In the RD retina, the primary source of aberrant activity is AII amacrine cell membrane oscillations, which are reliant on gap junction coupling (Trenholm et al., 2012; Choi et al., 2014). While the roles of AII amacrine cells and gap junctions in RD are becoming clear, it remains unclear whether gap junction coupling itself is altered. Physiological data have shown that targeting gap junctions with pharmacological agents eliminates aberrant activity, and provide indirect evidence that gap junctions may be excessively active (Toychiev et al., 2013a). Here, we begin to directly address this question by determining the extent of gap junction coupling in the RD retina. This is accomplished by using Neurobiotin tracer to visualize cell-to-cell coupling in *rd10* and *wt* retina. This approach is a useful measure of

both gap junction opening (Kothmann et al., 2009) and the degree of coupling (Bloomfield and Xin, 1997). Neurobiotin was applied using a cut-loading procedure (Ribelayga et al., 2008), and the degree of gap junction coupling was measured by the spread of Neurobiotin from its delivery site. Coupling was measured in both the ganglion cell layer (GCL, Fig. 3A) and the inner nuclear layer (INL, Fig. 3B). We found that *rd10* retinas (n = 5) indeed had increased coupling relative to *wt* (n = 7) in both the GCL (p = 0.006) and the INL (p = 0.03). MFA reduced coupling in *rd10* retinas in both the GCL (p = 0.016) and the INL (p = 0.03), as well as the *wt* GCL (p = 0.04), though not the *wt* INL (p = 0.12). Next, we pretreated retinas with MFA (100 μM) in bubbled Ames' medium for 10 min) to block gap junctions. In these conditions, *rd10* retinas (n = 4) did not differ from *wt* (n = 9) in either the GCL (p = 0.79) or the INL (p = 0.71). These data support the idea that gap junctions are excessively activated in RD. Next, we examined the proximal region of the inner nuclear layer, which is rich with AII amacrine cell bodies. Since AII amacrine cells are glycinergic, we labeled retinas for GlyT1 (Fig. 3C), a membrane glycine transporter (Zafra et al., 1995; Menger et al., 1998). In *wt* retina, Neurobiotin-labeled cells generally did not express GlyT1, while in *rd10* retina, cells weakly labeled with Neurobiotin expressed GlyT1.

It is established that Cx36-containing gap junctions mediate electrical connections among AII amacrine cells (Deans et al., 2002). Therefore, we hypothesized that elimination of Cx36 would reduce aberrant hyperactivity in RD mice. This has not been tested directly, since there is no specific pharmacological blocker of Cx36. Here, to selectively eliminate Cx36-containing gap junctions, we crossed *rd10* mice with Cx36 knockout mice (generously provided by Dr. David Paul of Harvard University). The resulting *rd10/Cx36*$^{-/-}$ mice exhibited photoreceptor degeneration and lacked the Cx36 protein that forms gap junctions, most notably in the lamina of inner plexiform layer enriched by the arboreal dendrites of AII amacrine cell (Fig. 4). We next recorded the inputs to both ON and OFF RGCs to determine the presence of aberrant activity in *rd10/Cx36*$^{-/-}$ mice, compared to *Cx36*$^{-/-}$ littermates, uncrossed *rd10* mice, and *wt* controls (Fig. 5A). In each animal strain, recordings were averaged across 10 RGCs in wholemount retinas from 5 mice. Aberrant activity was significantly reduced in *rd10/Cx36*$^{-/-}$ RGCs (Fig. 5C), in both ON (1.85 ± 1.13, n = 5, p < 0.0001) and OFF RGCs (1.35 ± 0.56, n = 5, p < 0.0001) compared to *rd10* (ON: 15.39 ± 3.75, n = 5, OFF: 25.78 ± 5.31, n = 5).

These data provide direct evidence for an essential role of Cx36-containing gap junctions in generating aberrant activity in RD. Since blocking gap junction inputs to AII amacrine cells can improve light responses in RD retina (Fig. 1), we next tested whether the genetic elimination of Cx36 would be sufficient to produce a similar improvement. Again using loose-patch mode, we monitored spiking activity from RGCs in *rd10/Cx36*$^{-/-}$ mice, *Cx36*$^{-/-}$ littermates, uncrossed *rd10* mice, and *wt* controls (Fig. 6A). Quantification (Fig. 6B) confirmed that *rd10/Cx36*$^{-/-}$ RGCs exhibited spontaneous spiking activity (9.76 ± 2.09 Hz, n = 19) that was significantly less than rd10 (102.66 ± 4.78 Hz, n = 25, p < 0.0001) and similar to wt RGCs (5.24 ± 0.70 Hz, n = 27, p = 0.99). Light responses were significantly greater than spontaneous activity in *rd10/Cx36*$^{-/-}$ RGCs (79.34 ± 5.57 Hz, p < 0.0001), while remaining lesser than light responses in *wt* (154.43 ± 7.36 Hz, p < 0.0001). Light responses of *rd10/Cx36*$^{-/-}$ RGCs did not significantly differ from *rd10* (107.22 ± 14.61 Hz, p = 0.079) or *Cx36*$^{-/-}$ RGCs (109.34 ± 11.10 Hz, p = 0.169).

Discussion

The goal of the present study was to provide a deeper insight into our understanding of the mechanisms of functional remodeling during progressive loss of photoreceptors both within the retina and how these changes might affect the retinal targets in the higher brain. This study has three major findings: (a) the aberrant activity within the degenerate retina impairs visual information processing. This negative effect is more prominent due to temporal bursting structure of the aberrant activity which is indistinguishable from the transient component of the evoked response; (b) the aberrant activity is transferred to the retinal targets in the higher brain, which suggest its role in visual perception in RD; (c) the altered coupling of the retinal amacrine cells via Cx36-containing gap junctions is essential for generating aberrant activity in RD.

The role for aberrant activity in RD

The concept of *structural* retinal remodeling has been largely known for several decades (Marc et al., 2003). The *functional* consequences of the photoreceptor cell loss on the surviving retinal tissue and their potential role in visual impairment and retinal repair, on the other hand, have begun to emerge relatively recently (Stasheff, 2008; Yee et al., 2012; Margolis et al., 2014). In particular, until few years ago, the loss of photoreceptors was considered the sole most important source of visual impairment in RD and the only target for repair. However, the finding of the emerging retinal hyperactivity has expanded this established paradigm to include the functional integrity of the inner retina as an important factor. Accumulating evidence suggests that RD is not simply a ‘loss of function’ disease, triggered by loss of sensory input, but rather an impairment that might be exacerbated by the addition or ‘gain of maladaptive function’. Indeed, we demonstrate that emerging aberrant activity has an effect of adding noise to the retinal information flow and creates an additional barrier which the weakened visual signal from surviving photoreceptors must now overcome (Fig. 1). Importantly, our findings demonstrate that this aberrant activity is not limited to retina and extends to its targets in the higher brain (Fig. 2). This is in agreement with an earlier report describing similar aberrant activity in both superior colliculus and visual cortex in another RD model, C57BL/6J-le *rd* mice (Drager and Hubel, 1978). This points to the stereotyped nature of the deficit across animals of different genetic strains. While earlier work has demonstrated that the blockade of aberrant activity can reduce the noise and improve fidelity of the retinal responses to visual stimulus (Toychiev et al., 2013a), it is for the future studies to determine whether this treatment in the retina will have a beneficial effect on the activity in the higher visual centers. Nevertheless, it is possible that therapies that consider functional changes in RD may prove to be the most effective in treating visual impairment.

Mechanisms of aberrant activity in RD

Aberrant activity in RD is primarily attributed to AII amacrine cell membrane oscillations, which are reliant on gap junction coupling (Trenholm et al., 2012; Choi et al., 2014). While the roles of AII amacrine cells and gap junctions in RD are becoming clear, it is unknown how mechanisms that regulate gap junctions lead to aberrant activity. Indeed, AII amacrine cells can be brought to oscillate in *wt* retina (Cembrowski et al., 2012), suggesting that

upstream retinal processes are modified during RD in a way that perturbs AII cell homeostasis, leading to membrane oscillations and aberrant activity. It remains unclear how gap junction-mediated interactions contribute to the generation of oscillatory potentials in AII amacrine cells, and how they affect the retinal network. Several models have emerged that address this question. According to one, a reduction in synaptic light-dependent input in RD leads to hyperpolarization in AII amacrine cells, leading directly to intrinsic membrane oscillations that drive aberrant activity; in this model, electrical coupling is relevant only insofar as it affects AII hyperpolarization (Choi et al., 2014). In another model, oscillations arise from heterogeneities in the respective electrical properties of AII amacrine cells and ON cone bipolar cells, which interact via gap junctions to induce an oscillatory network (Trenholm et al., 2012). Beyond having a significant role in generating aberrant activity, gap junctions are additionally essential for amplifying and propagating aberrant activity across the retinal network, by synchronizing the oscillations of large groups of cells spread across the retina (Menzler and Zeck, 2011; Margolis et al., 2014). Gap junction-mediated inputs to AII amacrine cells can come from both ON cone bipolar cells and from neighboring AII amacrine cells (Mills and Massey, 1995). Gap junctions in AII amacrine cells are primarily comprised of Cx36 (Deans et al., 2002). In this study, we provide direct evidence for the involvement of Cx36-containing gap junctions in aberrant activity. Since blocking gap junction inputs to AII amacrine cells can improve light responses in RD retina (Toychiev et al., 2013a), we crossed *rd10* mice with mice lacking Cx36, the major subunit in AII amacrine cell gap junctions (Deans et al., 2002). Despite having photoreceptor loss, RGCs in *rd10/Cx36*$^{-/-}$ mice exhibit reduced aberrant activity and had more robust light responses compared to *rd10* mice (Fig. 4, 5). Their activity, however, was higher when compared to *wt* RGCs. This could be due to elevated spontaneous rates in parent *Cx36*$^{-/-}$ mice (Blankenship et al., 2011). However, this elevated activity does not occur in bursts, which is the most disruptive part of aberrant activity in RD (Fig. 1, Toychiev et al., 2013a). The increased degree of gap junction coupling in *rd10* retina may contribute to this elevated activity. Interestingly, we observed this increase in both the INL and GCL (Fig. 3), indicating a role not only for amacrine cells, but also suggesting a role for gap junction-coupled ganglion cells. Indeed, the majority of ganglion cells in the retina are coupled in this way (Schubert et al., 2005b; Schubert et al., 2005a; Volgyi et al., 2005; Volgyi et al., 2009; Pan et al., 2010). This may contribute to correlated activity in RD retina (Menzler and Zeck, 2011; Volgyi et al., 2013).

Targeting gap junctions may prove to be a powerful approach in eliminating aberrant activity and restoring light responses in RD. Genetic defects associated with the disease typically do not have direct effects on the entire retina. Rather, a subset of dysfunctional cells degrades over time, while spreading destructive signals to neighboring cells. Recent work has suggested that this “death signal” may spread via gap junctions, which are a primary target of MFA in our approach (Akopian et al., 2014). Specifically, in both, *rd1* and *rd10* mice, the most commonly used experimental models of human retinitis pigmentosa, the primary deficit impacts rod photoreceptors. The death of cones is secondary and is believed to be triggered by rod degeneration. Therefore, in addition to its acute action via blockade of aberrant activity, it would be interesting to test in future studies whether chronic targeting of

gap junctions – for instance, by treating animals with MFA – may prevent these “death signals” from spreading and thus rescue vision by preventing secondary tissue damage.

Acknowledgments

This work was supported by NIH grant R01-EY020535 (B.T.S).

References

Akopian A, Atlasz T, Pan F, Wong S, Zhang Y, Volgyi B, Paul DL, Bloomfield SA. Gap junction466 mediated death of retinal neurons is connexin and insult specific: a potential target for neuroprotection. J Neurosci. 2014; 34:10582–10591. [PubMed: 25100592]

Blankenship AG, Hamby AM, Firl A, Vyas S, Maxeiner S, Willecke K, Feller MB. The role of neuronal connexins 36 and 45 in shaping spontaneous firing patterns in the developing retina. J Neurosci. 2011; 31:9998–10008. [PubMed: 21734291]

Bloomfield SA, Xin D. A comparison of receptive-field and tracer-coupling size of amacrine and ganglion cells in the rabbit retina. Vis Neurosci. 1997; 14:1153–1165. [PubMed: 9447695]

Cembrowski MS, Logan SM, Tian M, Jia L, Li W, Kath WL, Riecke H, Singer JH. The mechanisms of repetitive spike generation in an axonless retinal interneuron. Cell Rep. 2012; 1:155–166. [PubMed: 22832164]

Chang B, Hawes NL, Pardue MT, German AM, Hurd RE, Davisson MT, Nusinowitz S, Rengarajan K, Boyd AP, Sidney SS, Phillips MJ, Stewart RE, Chaudhury R, Nickerson JM, Heckenlively JR, Boatright JH. Two mouse retinal degenerations caused by missense mutations in the beta-subunit of rod cGMP phosphodiesterase gene. Vision Res. 2007; 47:624–633. [PubMed: 17267005]

Choi H, Zhang L, Cembrowski MS, Sabottke CF, Markowitz AL, Butts DA, Kath WL, Singer JH, Riecke H. Intrinsic Bursting of AII Amacrine Cells Underlies Oscillations in the rd1 Mouse Retina. J Neurophysiol. 2014

Deans MR, Gibson JR, Sellitto C, Connors BW, Paul DL. Synchronous activity of inhibitory networks in neocortex requires electrical synapses containing connexin36. Neuron. 2001; 31:477–485. [PubMed: 11516403]

Deans MR, Volgyi B, Goodenough DA, Bloomfield SA, Paul DL. Connexin36 is essential for transmission of rod-mediated visual signals in the mammalian retina. Neuron. 2002; 36:703–712. [PubMed: 12441058]

Drager UC, Hubel DH. Studies of visual function and its decay in mice with hereditary retinal degeneration. J Comp Neurol. 1978; 180:85–114. [PubMed: 649791]

Hofbauer A, Drager UC. Depth segregation of retinal ganglion cells projecting to mouse superior colliculus. J Comp Neurol. 1985; 234:465–474. [PubMed: 3988995]

Ivanova E, Toychiev AH, Yee CW, Sagdullaev BT. Optimized protocol for retinal wholemount preparation for imaging and immunohistochemistry. J Vis Exp. 2013:e51018. [PubMed: 24379013]

Kothmann WW, Massey SC, O'Brien J. Dopamine-stimulated dephosphorylation of connexin 36 mediates AII amacrine cell uncoupling. J Neurosci. 2009; 29:14903–14911. [PubMed: 19940186]

Marc RE, Jones BW, Watt CB, Strettoi E. Neural remodeling in retinal degeneration. Prog Retin Eye Res. 2003; 22:607–655. [PubMed: 12892644]

Marc RE, Jones BW, Anderson JR, Kinard K, Marshak DW, Wilson JH, Wensel T, Lucas RJ. Neural reprogramming in retinal degeneration. Invest Ophthalmol Vis Sci. 2007; 48:3364–3371. [PubMed: 17591910]

Margolis DJ, Gartland AJ, Singer JH, Detwiler PB. Network oscillations drive correlated spiking of ON and OFF ganglion cells in the rd1 mouse model of retinal degeneration. PLoS One. 2014; 9:e86253. [PubMed: 24489706]

Mazzoni F, Novelli E, Strettoi E. Retinal ganglion cells survive and maintain normal dendritic morphology in a mouse model of inherited photoreceptor degeneration. J Neurosci. 2008; 28:14282– 14292. [PubMed: 19109509]

Menger N, Pow DV, Wassle H. Glycinergic amacrine cells of the rat retina. J Comp Neurol. 1998; 401:34–46. [PubMed: 9802699]

Menzler J, Zeck G. Network oscillations in rod-degenerated mouse retinas. J Neurosci. 2011; 31:2280–2291. [PubMed: 21307264]

Mills SL, Massey SC. Differential properties of two gap junctional pathways made by AII amacrine cells. Nature. 1995; 377:734–737. [PubMed: 7477263]

O'Leary DD, McLaughlin T. Mechanisms of retinotopic map development: Ephs, ephrins, and spontaneous correlated retinal activity. Prog Brain Res. 2005; 147:43–65. [PubMed: 15581697]

Pan F, Paul DL, Bloomfield SA, Volgyi B. Connexin36 is required for gap junctional coupling of most ganglion cell subtypes in the mouse retina. J Comp Neurol. 2010; 518:911–927. [PubMed: 20058323]

Ribelayga C, Cao Y, Mangel SC. The circadian clock in the retina controls rod-cone coupling. Neuron. 2008; 59:790–801. [PubMed: 18786362]

Sagdullaev BT, McCall MA, Lukasiewicz PD. Presynaptic inhibition modulates spillover, creating distinct dynamic response ranges of sensory output. Neuron. 2006; 50:923–935. [PubMed: 16772173]

Sagdullaev BT, Aramant RB, Seiler MJ, Woch G, McCall MA. Retinal transplantation-induced recovery of retinotectal visual function in a rodent model of retinitis pigmentosa. Invest Ophthalmol Vis Sci. 2003; 44:1686–1695. [PubMed: 12657610]

Schubert T, Maxeiner S, Kruger O, Willecke K, Weiler R. Connexin45 mediates gap junctional coupling of bistratified ganglion cells in the mouse retina. J Comp Neurol. 2005a; 490:29–39. [PubMed: 16041717]

Schubert T, Degen J, Willecke K, Hormuzdi SG, Monyer H, Weiler R. Connexin36 mediates gap junctional coupling of alpha-ganglion cells in mouse retina. J Comp Neurol. 2005b; 485:191–201. [PubMed: 15791644]

Stasheff SF. Emergence of sustained spontaneous hyperactivity and temporary preservation of OFF responses in ganglion cells of the retinal degeneration (rd1) mouse. J Neurophysiol. 2008; 99:1408–1421. [PubMed: 18216234]

Toychiev AH, Ivanova E, Yee CW, Sagdullaev BT. Block of gap junctions eliminates aberrant activity and restores light responses during retinal degeneration. J Neurosci. 2013a; 33:13972–13977. [PubMed: 23986234]

Toychiev AH, Sagdullaev B, Yee CW, Ivanova E, Sagdullaev BT. A time and cost efficient approach to functional and structural assessment of living neuronal tissue. J Neurosci Methods. 2013b; 214:105–112. [PubMed: 23370309]

Trenholm S, Borowska J, Zhang J, Hoggarth A, Johnson K, Barnes S, Lewis TJ, Awatramani GB. Intrinsic oscillatory activity arising within the electrically coupled AII amacrine-ON cone bipolar cell network is driven by voltage-gated Na+ channels. J Physiol. 2012; 590:2501–2517. [PubMed: 22393249]

Volgyi B, Chheda S, Bloomfield SA. Tracer coupling patterns of the ganglion cell subtypes in the mouse retina. J Comp Neurol. 2009; 512:664–687. [PubMed: 19051243]

Volgyi B, Abrams J, Paul DL, Bloomfield SA. Morphology and tracer coupling pattern of alpha ganglion cells in the mouse retina. J Comp Neurol. 2005; 492:66–77. [PubMed: 16175559]

Volgyi B, Pan F, Paul DL, Wang JT, Huberman AD, Bloomfield SA. Gap junctions are essential for generating the correlated spike activity of neighboring retinal ganglion cells. PLoS One. 2013; 8:e69426. [PubMed: 23936012]

Yee CW, Toychiev AH, Sagdullaev BT. Network deficiency exacerbates impairment in a mouse model of retinal degeneration. Front Syst Neurosci. 2012; 6:8. [PubMed: 22383900]

Yee CW, Toychiev AH, Ivanova E, Sagdullaev BT. Aberrant synaptic input to retinal ganglion cells varies with morphology in a mouse model of retinal degeneration. J Comp Neurol. 2014; 522:4085–4099. [PubMed: 25099614]

Zafra F, Aragon C, Olivares L, Danbolt NC, Gimenez C, Storm-Mathisen J. Glycine transporters are differentially expressed among CNS cells. J Neurosci. 1995; 15:3952–3969. [PubMed: 7751957]

Highlights

a. The aberrant activity within the degenerate retina impairs visual information processing. This negative effect is more prominent due to temporal bursting structure of the aberrant activity which is indistinguishable from the transient component of the evoked response;

b. The aberrant activity is transferred to the retinal targets in the higher brain, which suggest its role in visual perception in RD;

c. The altered coupling of the retinal amacrine cells via Cx36-containing gap junctions is essential for generating aberrant activity in RD.

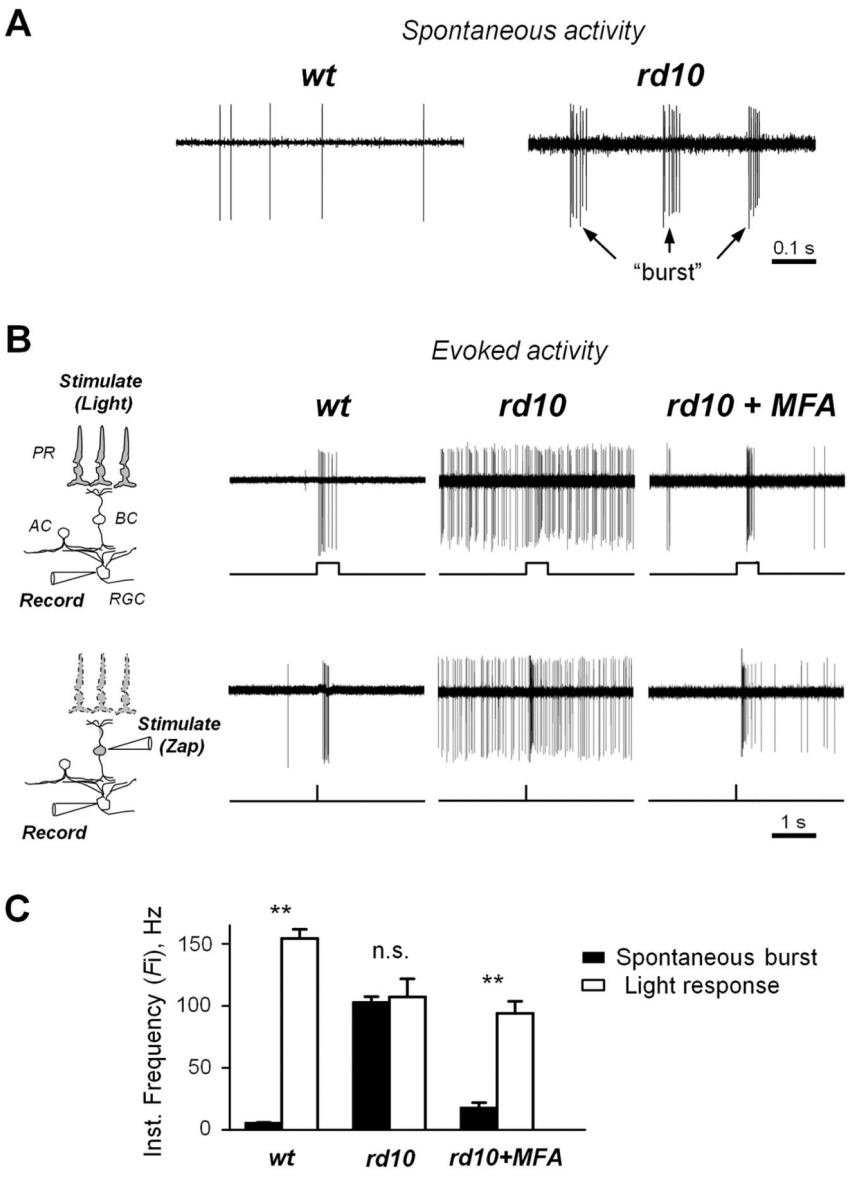

Figure 1.

Aberrant activity following photoreceptor cell death reduces the fidelity of evoked signals within the surviving retina. **A.** Retinal ganglion cells in degenerate retina spontaneously fire intermittent "bursts" of action potentials. **B.** Series of light-evoked (P40 mice, top) and electrically-evoked 'zap' (P140 mice, bottom) responses from rd10 RGCs before (center) and after treatment (right) with meclofenamic acid (MFA, 50 μM), and wt controls (left). Block of gap junctions eliminates aberrant hyperactivity, improving discrimination of evoked responses in RD. Diagrams illustrate the experimental approach to test photoreceptor-dependent (using light) and photoreceptor-independent (using focal electrical 'zap' pulse) signal transmission in the retina. Abbreviations: PR - photoreceptor cell, BC - bipolar cell, AC - amacrine cell, RGC – retinal ganglion cell. **C.** Aberrant bursts of spikes are indistinguishable from light-evoked responses in RD. Histogram shows instantaneous frequency rates within spontaneous bursts and the transient portion of light-evoked

responses in wt controls and rd10 RGCs before and after treatment with MFA. Error bars represent SEM. **p < 0.001, n.s. – not significant.

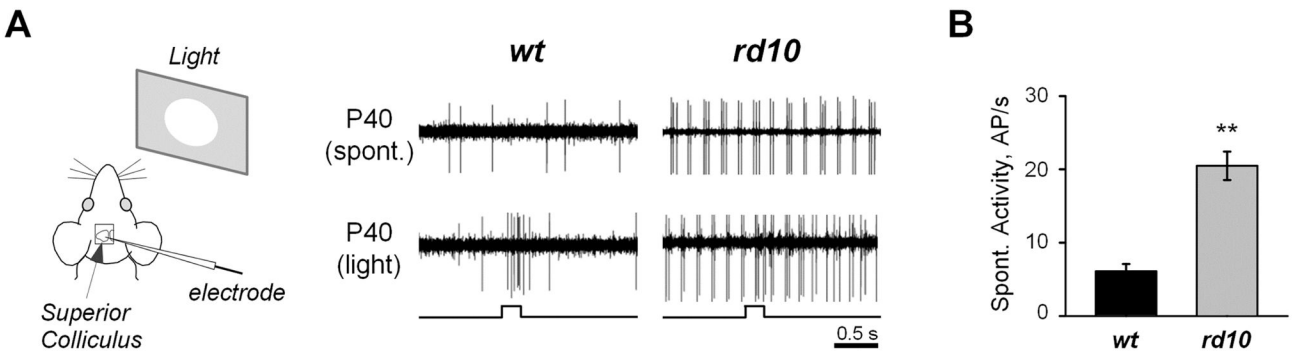

Figure 2.

Aberrant retinal activity impairs light responses in retinotectal projections in the higher brain. **A.** In vivo recordings of spontaneous activity and responses to retinal light stimulation from superior colliculus were performed as illustrated in the left panel, in anesthetized wt and rd10 mice. In contrast to wt, neurons in superficial layer of superior colliculus in rd10 mice are hyperactive – evidence that aberrant retinal activity impairs visual processing in higher visual centers. **B.** Quantification of spontaneous aberrant activity in wt and RD mice. The data shows mean firing activity in cells in superficial layer of the superior colliculus across 29 recording sites in 3 individual animals for each wt and RD mice. AP/s – action potentials per second. Error bars represent SEM. **p < 0.001.

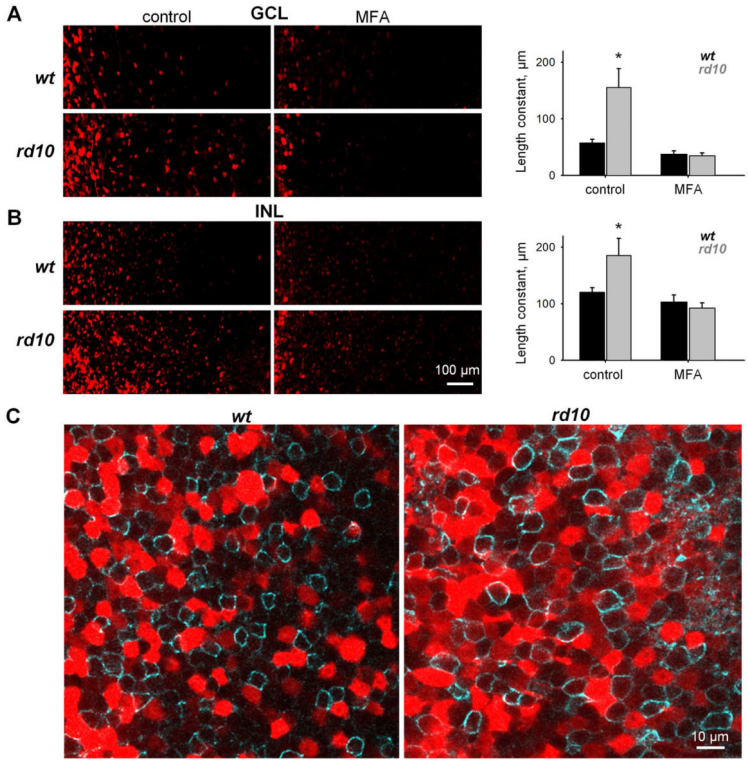

Figure 3.

Increased coupling of retinal cells in rd10 assessed by measuring Neurobiotin spread after cut-loading. Living retinas were dissected from the eye and cut into quarters. Each quarter was attached to a filter and cut by a razor blade dipped in Neurobiotin. After fixation, Neurobiotin was visualized with Streptavidin-Cy3. In all images, the cut is on the left side. **A-B.** Left panels: Coupling of cells in the ganglion cell layer (GCL, A) and at the proximal region of the inner nuclear layer (INL, B) in control solution and in the presence of MFA. Right panels: Histograms summarizing the degree of gap junction coupling as measured by the length constant of Neurobiotin spread from the cut site. In control conditions, more coupling was found in both layers of rd10 retina. In the presence of MFA, coupling in rd10 was decreased to wt levels. **C.** Single confocal section through the INL of the retinas double-labeled for Neurobiotin (red) and the glycine transporter GlyT1 (cyan). Weakly labeled red cells were GlyT1-positive. They are most likely to be narrow-field amacrine cells labeled by Neurobiotin propagated via gap junctions. Bright red cells were presumably wide-field GABAergic amacrine cells that directly picked up Neurobiotin by their long dendrites. The number of Neurobiotin-labeled glycinergic cells was much higher in rd10 retinas.

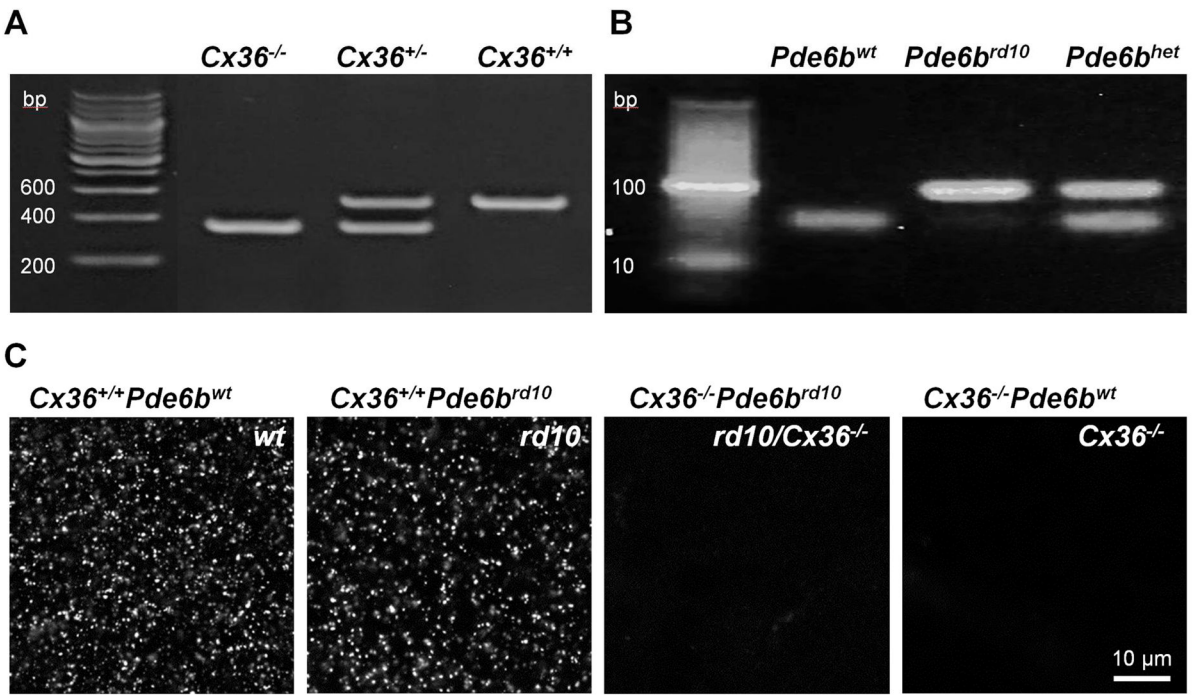

Figure 4.

Generation and identification of rd10/Cx36$^{-/-}$ mice. **A.** PCR products from genotyping for Cx36. wt (Cx36$^{+/+}$) DNA produce a 533 bp band, in contrast to a 360 bp band in the Cx36 knockout (Cx36$^{-/-}$). **B.** The rd10 (Pde6b^{rd10}) mutation were genotyped by PCR for the β-subunit of the rod-specific phosphodiesterase gene mutated in this mouse model. After amplification of the gene from DNA of wt and rd10 mice, digestion of PCR-amplified products was performed by NarI enzyme. Only wt (Pde6b^{wt}) DNA could be digested, resulting in two adjacent bands at ~50 bp, while rd10 DNA produces a 100 bp band. **C.** The absence of Cx36 in Cx36$^{-/-}$ mice was further confirmed by immunolabeling retinal wholemounts for Cx36. Single confocal sections at the ON sublamina of the inner plexiform layer exhibited punctate staining in mice genotyped as expressing Cx36 (Cx36$^{+/+}$) but not mice determined to have the knockout (Cx36$^{-/-}$).

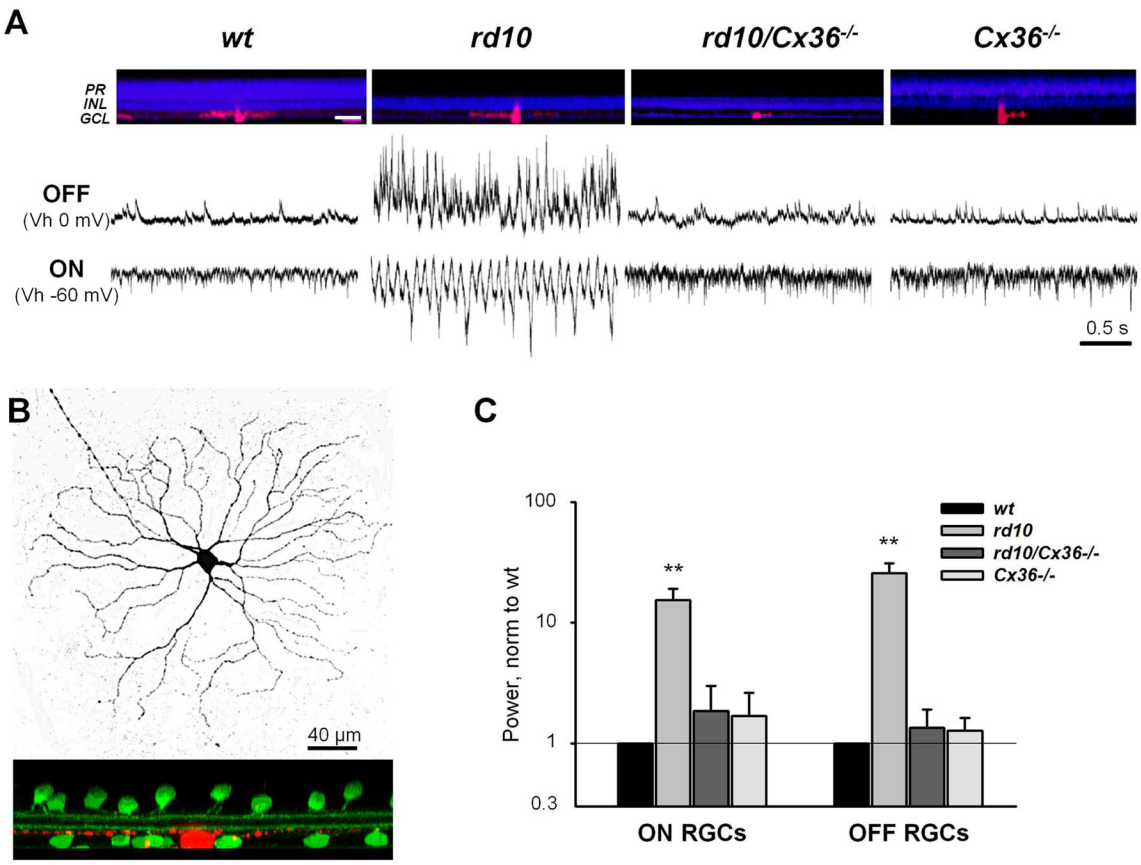

Figure 5.

Genetic deletion of Cx36-containing gap junctions reduces hyperactivity in RD. **A.** Retinal cross sections from age-matched experimental mice (top). Cell layers are labeled with nuclear stain (TO-PRO-1, blue) and recorded RGCs are filled with Alexa (red). Aberrant activity typical of rd10 ON and OFF RGCs is diminished in rd10/Cx36$^{-/-}$ RGCs even following photoreceptor loss. Abbreviations: PR – photoreceptor cell layer, INL – inner nuclear layer, and GCL – ganglion cell layer. Scale bar - 50 µm. **B.** Representative ON RGC backfilled with Alexa 568 (red) following the recording procedure. The depth of stratification is determined relative to ChAT bands (green). **C.** Quantification of aberrant activity in wt, rd10, rd10/Cx36$^{-/-}$ and Cx36$^{-/-}$ RGCs. Spontaneous excitatory (sEPSCs, ON RGCs) and inhibitory (sIPSCs, OFF RGCs) activity were estimated as power of integrated current. To reduce contribution of DC-shift, currents were adjusted for baseline. Error bars represent S.E.M. **p < 0.001.

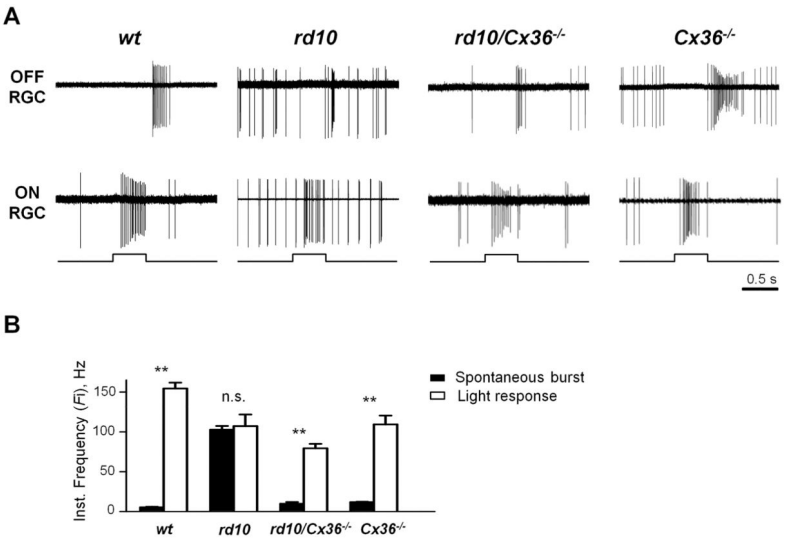

Figure 6.

Genetic deletion of Cx36 reduces hyperactivity in RD retina output and restores discrimination of responses to light. **A.** Aberrant activity is diminished in rd10/Cx36$^{-/-}$ (P45) in both ON and OFF RGCs. **B.** Cx36 knockout restores differentiation between spontaneous bursts and light responses in RD. Histogram shows instantaneous frequency rates within spontaneous bursts and the transient portion of light-evoked responses in RGCs from wt controls, uncrossed rd10s, rd10/Cx36$^{-/-}$ mice, and Cx36$^{-/-}$ littermates. Error bars represent SEM. **p < 0.001, n.s. – not significant.